COBEM 2021 26th International Congress of Mechanical Engineering
ABCM Associação Brasileira de Engenharia e Ciências Mecânicas
November 22-26, 2021, Virtual Congress, Brazil

COB-2021-1008
ON THE USE OF NUMERICAL APPROXIMATE METHODS FOR PREDICTING THE HEAT TRANSFER DURING THE ATMOSPHERIC RE-ENTRY OF A BLUNT BODY

Filipe Eduardo da Silva
Francisco Augusto Aparecido Gomes
Federal University of Technology – Paraná, Pato Branco, Brazil
filipe.1998@alunos.utfpr.edu.br
franciscogomes@utfpr.edu.br

Abstract. *This work objective is to evaluate the heat transfer in the stagnation point of a space vehicle with a blunt body geometry during its entrance into the atmosphere. These data are extremely important for the development of a thermal protection system. The five approximate methods used were: Tauber, Van Driest, Fay-Riddell, Detra-Hidalgo, and Sutton-Graves, all these methods were implemented in a programming language known as Fortran 90/95 along with the Standard Atmosphere of 1976 and other four methods to obtain the air properties after the normal shock wave, where one of these methods is the perfect gas model and the other three are the thermodynamic equilibrium. The integration of the heat flux with respect to the trajectory time results in the heat load, in the present work it was considered three different wall temperatures in the vehicle: 1000 K, 2000K, and 3000 K. Lastly, it's shown the graphics of the heat flux with respect to trajectory time, and then a comparison between the heat load for each method. The heat flux method that presented the highest values of heat load was Detra-Hidalgo with 264.0 MJ/m^2 for a wall temperature of 1000 K and 209.0 MJ/m^2 in a 3000 K wall temperature.*

Keywords: *Aerothermodynamics, Atmospheric Entry, Heat Transfer, Stagnation Point, Thermodynamic Equilibrium.*

1. INTRODUCTION

Whenever a space vehicle (SV) is re-entering the atmosphere, it becomes exposed to high temperatures (Regan and Anandakrishnan, 1993), therefore developing a thermal protection system (TPS) is a must, but first is necessary to evaluate the maximum value of heat flux, along with the heat load, data such as this are crucial for design aspects.

There are two ways of analysing the heating problem in the stagnation point of an SV re-entering the atmosphere, by using computational fluid dynamics (CFD) or approximate methods. Even though CFD simulations are excellent in outputting results, it takes a lot of time to converge, meanwhile, approximate methods show good results with a time convergence lower (Anderson Junior, 2006).

Considering the information above, this work's main objective is to show how data are obtained about the aerodynamic heating that happens in the stagnation point of the Brazilian microsatellite SARA while considering the approximate methods. It is important to mention that this numerical analysis was accomplished through the programming language Fortran 90/95 (Chapman, 2018), and is restricted to a space vehicle with a blunt body geometry (Anderson Junior, 2006), re-entering with a 0º angle of attack.

Through the trajectory is possible to obtain the properties of the air at any point of altitude using the Standard Atmosphere of 1976. Since in most of the trajectory time the SV Mach number is higher than 1, a shock wave is going to be formed ahead of the SV nose, this phenomenon alters the air properties and it needs to be accounted for, this can be done through the perfect gas model or the thermodynamic equilibrium.

The last step consists of applying the convective heat transfer methods or approximate methods, which were: Tauber, Van Driest, Fay-Riddell, Detra-Hidalgo, and Sutton-Graves. The approach using Detra-Hidalgos's method presented the highest values of heat flux and heat load for all the three wall temperatures tested.

2. METHODS

To come to the heat flux values and compare them, it is necessary to first obtain the properties of the air before and after the normal shock wave as represented in Fig. 1. The only approach that uses the properties directly from the thermodynamic equilibrium is Fay-Riddell's method.

Over the years, one method of obtaining the high-temperature properties of air through the thermodynamic equilibrium suffered three modifications. The difference between every new version was that the polynomial relation responsible for returning the data received a higher order. All three variants were used in this work so that it was also possible to compare the results.

Figure 2 shows the trajectory of the microsatellite SARA (Toro *et al.*, 2004). This SV starts its entrance about 300 km of altitude with a velocity of around 7600 m/s, it is also notable that it reaches the maximum velocity at 93 km of altitude or with a time trajectory of 1475 seconds. The total trajectory time is close to 2000 s.

The streamline conditions shown in Fig. 1 are achieved by using the trajectory information and the U.S. Standard Atmosphere of 1976 (COESA, 1976). It is important to mention that the SARA nose radius (R_{SV}) is 0.2678 m, and it was only considered the aerodynamic heating below 92 km of altitude.

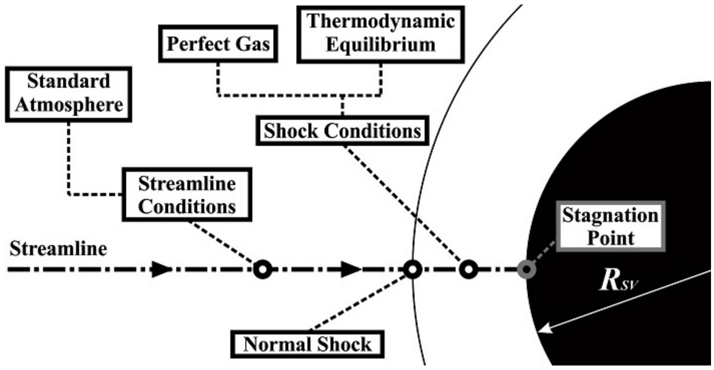

Figure 1. Schematic representation of the properties of air and shock wave.

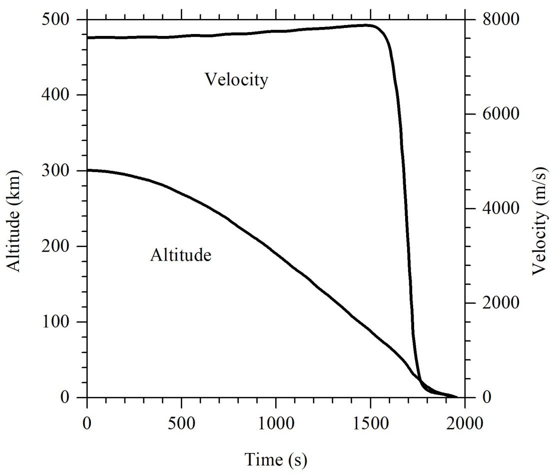

Figure 2. Trajectory of the microsatellite SARA (Toro *et al.*, 2004).

2.1 ATMOSPHERIC MODEL OF 1976

Regan and Anandakrishnan (1993) described how to use the U.S. Standard Atmosphere of 1976 (COESA, 1976), this atmospheric model will provide information such as temperature, pressure, and density as a function of altitude. In this model, the atmosphere was divided into layers. The behave of the temperature as a function of altitude will be different in every layer and the rate of change between these two variables is known as thermal lapse rate, or,

$$L_{Zi} = \left.\frac{dT}{dZ}\right|_i , \tag{1}$$

at Eq. 1, T is the molecular temperature (K), Z is the geometric altitude (km) and the subscript "i" denotes the layer.

The temperature T_1, which is the streamline temperature, or the temperature before the normal shock is calculated with the following equation:

$$T_1 = T_i + L_{Zi} \cdot (Z - Z_i), \tag{2}$$

Z (km) is the altitude value at which the SV is at a specific time. Once the thermal lapse rate is equal to 0, the temperature T_1 has the same value as T_i, meanwhile P_1 (N/m^2) and ρ_1 (kg/m^3) are calculated by:

$$P_1 = P_i \cdot exp\left[-\left(\frac{g \cdot (Z - Z_i)}{\bar{R} \cdot T_i}\right) \cdot \left(1 - \frac{b}{2} \cdot (Z - Z_i)\right)\right], \tag{3}$$

$$\rho_1 = \rho_i \cdot exp\left[-\left(\frac{g \cdot (Z - Z_i)}{\bar{R} \cdot T_i}\right) \cdot \left(1 - \frac{b}{2} \cdot (Z - Z_i)\right)\right]. \tag{4}$$

Analysing Eq. 3 and Eq. 4, P_i (N/m^2) and ρ_i (kg/m^3) are the pressure and density at specific layer, g represents the gravitational acceleration with approximate value of 9.81 m/s^2, $\bar{R}$ is the universal gas constant (8314.0 J/kmol·K) and b has a constant value of 3.139·10^{-7}/m. Whenever $L_{Zi} \neq 0$, T_1 must be calculated using Eq. 2, meanwhile P_1 and ρ_1 are found through:

$$P_1 = P_i \cdot \left[\left(\frac{L_{Zi}}{\bar{R} \cdot T_i}\right) \cdot (Z - Z_i) + 1\right]^{-\left[\left(\frac{g}{\bar{R} \cdot L_{Zi}}\right) \cdot \left(1 + b\left(\frac{T_i}{L_{Zi}} - Z_i\right)\right)\right]} \cdot exp\left[\left(\frac{g \cdot b}{\bar{R} \cdot L_{Zi}}\right) \cdot (Z - Z_i)\right], \tag{5}$$

$$\rho_1 = \rho_i \cdot \left[\left(\frac{L_{Zi}}{\bar{R} \cdot T_i}\right) \cdot (Z - Z_i) + 1\right]^{-\left[\left(\frac{g}{\bar{R} \cdot L_{Zi}}\right) \cdot \left(\frac{\bar{R} \cdot L_{Zi}}{g} + 1 + b\left(\frac{T_i}{L_{Zi}} - Z_i\right)\right)\right]} \cdot exp\left[\left(\frac{g \cdot b}{\bar{R} \cdot L_{Zi}}\right) \cdot (Z - Z_i)\right]. \tag{6}$$

Table 1 indicates the information necessary to use the previous equations. Since this work is limited to 92 km of altitude, to obtain the temperature (T_1) and the thermal lapse rate (L_{Zi}) from 91 km until 110.0 km of altitude,

$$T_1 = T_c + A_c \cdot \left[1 - \left(\frac{Z - Z_8}{a_c}\right)^2\right]^{1/2}, \tag{7}$$

$$\frac{dT}{dZ} = -\frac{A_c}{a_c}\left(\frac{Z - Z_8}{a_c}\right)^2 \cdot \left[1 - \left(\frac{Z - Z_8}{a_c}\right)^2\right]^{-1/2}, \tag{8}$$

where T_c, A_c and a_c are constants, and its values are 263.1902 K, -76.3232 K and -19.9429 km respectively.

Table 1. Atmosphere layers information up to 91 km of geometric altitude (Regan and Anandakrishnan, 1993).

Layer index	Geometric altitude Z (km)	Molecular temperature T_i (K)	Thermal lapse rate L_{Zi} (K/km)
0	0.0	288.150	-6.5
1	11.0102	216.650	0.0
2	20.0631	216.650	+1.0
3	32.1619	228.650	+2.8
4	47.3501	270.650	0.0
5	51.4125	270.650	-2.7
6	71.8020	214.650	-2.0
7	86.0	186.946	0.0
8	91.0	186.946	

The speed of sound (v_s) in m/s and Mach number (M_1) are found through:

$$v_s = (\gamma \cdot R_{air} \cdot T_1)^{0.5}, \tag{9}$$

$$M_1 = \frac{v_1}{v_s}, \tag{10}$$

where the heat capacity ratio γ assumes the constant value of 1.4 and R_{air} represents the constant of the air with an approximate value of 287.05 J/kg·K, v_1 is the trajectory speed (m/s).

2.2 PROPERTIES OF THE AIR AFTER THE SHOCK WAVE

As demonstrated by Anderson Junior (2003), the air properties after the normal shock can be found considering the perfect gas model, these correlations will only vary with the values of the properties before the normal shock, so,

$$\frac{\rho_2}{\rho_1} = \frac{(\gamma + 1) \cdot M_1^2}{2 + (\gamma - 1) \cdot M_1^2}, \tag{11}$$

$$\frac{P_2}{P_1} = 1 + \frac{2 \cdot \gamma}{\gamma + 1} \cdot (M_1^2 - 1), \tag{12}$$

$$\frac{T_2}{T_1} = \left[1 + (M_1^2 - 1) \cdot \frac{2 \cdot \gamma}{\gamma + 1}\right] \cdot \left[\frac{2 + (\gamma - 1) \cdot M_1^2}{(\gamma + 1) \cdot M_1^2}\right], \tag{13}$$

for this model, γ still has a constant value of 1.4. In the Eq. 11, ρ_2 (N/m^2) will be the density after the normal shock. The same is done in Eq. 12 and Eq. 13, where the variables P_2 and T_2 represent the pressure and temperature after the normal shock.

Figure 3 establishes a representation of these variables, whereas a similar illustration is found in the book of Anderson Junior (2006).

The high values of Mach number which the SV experience create a very strong shock wave due to its blunt body geometry, this turns the region ahead of the nose into a high temperature zone, the problem relies on the fact that at high temperatures the present molecules in the air such as oxygen and nitrogen start to dissociate or even ionize (Anderson Junior, 2006), this reaction of breaking molecules consumes a great amount of energy to the extent that the temperature in that point will be lower than the values presented in the perfect gas model since it does not account for these reactions.

Using the thermodynamic equilibrium is possible to find more realistic data about the properties of the air after the normal shock (Anderson Junior, 2006). All this can be made through tabulated data and polynomial correlations as demonstrated in the works of Tannehill and Mohling (1972), Tannehill and Mugge (1974) and Srinivasan *et al.* (1987), the difference between these works is that in every last one, an even higher degree polynomial correlations was created.

Velocity ($v_{\bar{2}}$), enthalpy ($h_{\bar{2}}$) and density ($\rho_{\bar{2}}$) represented in Fig. 3 are found from momentum, energy equations and continuity (Anderson Junior, 2003), however pressure ($P_{\bar{2}}$) and temperature ($T_{\bar{2}}$) are obtained as functions of other two properties.

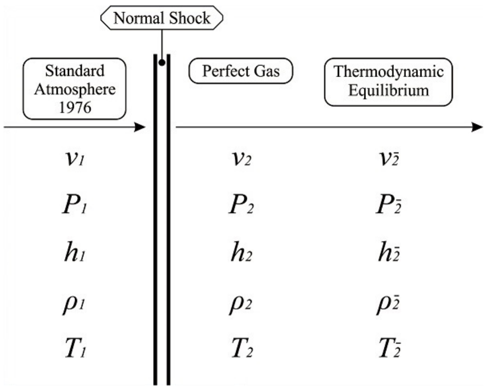

Figure 3. Representation of the properties to be calculated.

The procedure for the use of any thermodynamic equilibrium model mentioned before is very similar, therefore, this work will only describe the implementation of the newest model, which is the one presented in 1987 (Srinivasan *et al.*, 1987). The steps shown below are also present in the book "Hypersonic and high-temperature gas dynamics" (Anderson Junior, 2006). Firstly, the flow is considered to be one-dimensional and steady, this way:

$$v_{\bar{2}} = \frac{\rho_1 \cdot v_1}{\rho_{\bar{2}}}, \tag{14}$$

$$P_{\bar{2}} = P_1 + \rho_1 \cdot v_1^2 \cdot \left(1 - \frac{\rho_1}{\rho_{\bar{2}}}\right), \tag{15}$$

$$h_{\bar{2}} = h_1 + \frac{v_1^2}{2} \cdot \left[1 - \left(\frac{\rho_1}{\rho_{\bar{2}}}\right)^2\right]. \tag{16}$$

For this model, pressure is determined as a function of internal energy and density, or:

$$P_{\bar{2}} = P(e_{\bar{2}}, \rho_{\bar{2}}), \tag{17}$$

$$P_{\bar{2}} = \rho_{\bar{2}} \cdot e_{\bar{2}} \cdot (\tilde{\gamma}_{1987} - 1). \tag{18}$$

The heat capacity ratio for the thermodynamic equilibrium is not constant, this way, $\tilde{\gamma}_{1987}$ is calculated using the following polynomial correlation:

$$\begin{aligned} \tilde{\gamma}_{1987} = {} & a_1 + a_2 Y + a_3 Z + a_4 YZ + a_5 Y^2 + a_6 Z^2 + a_7 Y^2 Z + a_8 YZ^2 + a_9 Y^3 + a_{10} Z^3 + \\ & (a_{11} + a_{12} Y + a_{13} Z + a_{14} YZ + a_{15} Y^2 + a_{16} Z^2 + a_{17} Y^2 Z + a_{18} YZ^2 + a_{19} Y^3 + a_{20} Z^3)/ \\ & [1 \pm exp(a_{21} + a_{22} Y + a_{23} Z + a_{24} YZ)], \end{aligned} \tag{19}$$

in this equation, $a_1, a_2, ..., a_{24}$ are constants that are found in tabulated data (Srinivasan *et al.*, 1987) and depend on the values of Y and Z:

$$Y = \log_{10}(\rho_{\bar{2}}/\rho_0), \tag{20}$$

$$Z = \log_{10}(e_{\bar{2}}/78410.4), \tag{21}$$

in Eq. 19 the signal adopted in $\pm$ will depend on the constants that are being used, ρ_0 in Eq. 20 is the density at 273.15 K and 101.325 kN/m^2.

To evaluate the temperature ($T_{\bar{2}}$), Eq. 22 is used, where Z is given by Eq. 23, therefore:

$$\begin{aligned}\log_{10}(T_{\bar{2}}/273.15)_{1987} = {} & b_1 + b_2Y + b_3Z + b_4YZ + b_5Y^2 + b_6Z^2 + b_7Y^2Z + b_8YZ^2 + b_9Y^3 + b_{10}Z^3 + \\ & (b_{11} + b_{12}Y + b_{13}Z + b_{14}YZ + b_{15}Y^2 + b_{16}Z^2 + b_{17}Y^2Z + \\ & b_{18}YZ^2 + b_{19}Y^3 + b_{20}Z^3)/[1 \pm exp(b_{21} + b_{22}Y + b_{23}Z + b_{24}YZ)],\end{aligned} \tag{22}$$

$$Z = X - Y, \tag{23}$$

$$X = \log_{10}(P_{\bar{2}}/101325). \tag{24}$$

Since the value of $\rho_{\bar{2}}$ is not known, a numerical routine must be created in order to obtain these properties (Anderson Junior, 2006). First, the ratio $\rho_1/\rho_{\bar{2}}$ is assume to be a low value such as 0.1, with that, pressure ($P_{\bar{2}}$) and enthalpy ($h_{\bar{2}}$) are calculated from Eq. 15 and Eq. 16. The next step is obtain the internal energy ($e_{\bar{2}}$) from,

$$e_{\bar{2}} = h_{\bar{2}} - (P_{\bar{2}}/\rho_{\bar{2}}), \tag{25}$$

now with the values of Y and Z from Eq. 20 and Eq. 21 the heat capacity ratio ($\tilde{\gamma}_{1987}$) is calculated and a new value of $\rho_{\bar{2}}$ is determined with Eq. 18, with all that, a new ratio $\rho_1/\rho_{\bar{2}}$ is generated, this entire process must be repeated from 3 to 5 times so that a good convergence is acquired. With all these properties calculated, the temperature ($T_{\bar{2}}$) from Eq. 22 can be obtained.

3. APPROXIMATE METHODS AND HEAT LOAD

Before describing the convective heat transfer approximate methods is of great importance to define the wall temperature (T_w) of the TPS, in this work, T_w is considered to be constant over the entire trajectory and assume three possible values: 1000 K, 2000 K, and 3000 K.

3.1 TAUBER

Equation 26 was proposed by Tauber *et al.* (1986), where the heat flux $\dot{q}_t$ is given in W/cm^2, N and M are constants that if the stagnation point is being considered, assume the values of 0.5 and 3 respectively. C is determined using Eq. 27, ρ_1 needs to be in kg/m^3 and v_1 must be given in m/s.

$$\dot{q_t} = {\rho_1}^N \cdot {v_1}^M \cdot C. \tag{26}$$

$$C = 1.83 \cdot 10^{-8} \cdot R_{SV} \cdot (1 - h_w/h_o). \tag{27}$$

In Eq. 27, R_{SV} represents the nose radius of SARA (m), also shown in Fig. 1. h_o (J/kg) and h_w (J/kg) are the total and wall enthalpy, thus,

$$h_o = h_1 + \frac{{v_1}^2}{2}, \tag{28}$$

$$h_w = c_p \cdot T_w, \tag{29}$$

at Eq. 28, h_1 is the air enthalpy (J/kg) before the normal shock, and c_p in Eq. 29 is the specific heat capacity with a constant value of 1004.5 J/kg·K. This approach considers a fully catalytic surface.

3.2 VAN DRIEST

Van Driest (1956) suggested the following expression to obtain the heat transfer q_{vd} (W/m^2) in a spherical nose and laminar flow,

$$\dot{q_{vd}} = 0.763 \cdot Pr^{-0.6} \cdot (\rho_2\mu_2)^{1/2} \cdot \sqrt{\frac{dv_2}{dx}} \cdot (h_{aw} - h_w), \tag{30}$$

Pr is the Prandtl number with a constant value of 0.71, the coefficient of viscosity μ_2 (kg/m·s) is found through the Sutherland equation (Anderson Jr., 2006). In Eq. 30, dv_2/dx and h_{aw} are the velocity gradient and adiabatic wall enthalpy (J/kg),

$$\frac{dv_2}{dx} = \frac{1}{R_{SV}}\sqrt{\frac{2 \cdot (P_2 - P_1)}{\rho_2}}, \tag{31}$$

$$h_{aw} = h_2 + r(h_o - h_2), \tag{32}$$

h_2 is the enthalpy after the normal shock in J/kg and r is the recovery factor which represents the square root of the Prandtl number.

3.3 SUTTON-GRAVES

Another simple way of finding the heat transfer in the stagnation point is represented in Eq. 33, where A is a constant determined by Sutton-Graves (Alber, 2012) with an approximate value of $1.75{\cdot}10^{-4}$ kg$^{0.5}$/m. q_{sg} will be given in W/m^2. This method is valid for wall temperatures from 300 K until 1111 K and pressures of 101.325 N/m^2 up to $1.013{\cdot}10^7$ N/m^2.

$$\dot{q_{sg}} = \frac{A}{\sqrt{R_{SV}}} \cdot {\rho_1}^{0.5} \cdot {v_1}^3. \tag{33}$$

3.4 DETRA-HIDALGO

Equation 34 was adjusted so that Detra and Hidalgo (1961) method will work with the units of R_{SV} and v_1 in m and m/s respectively, the result of this equation ($\dot{q_{dh}}$) is W/cm^2, ρ_o represents the air density at ground level (kg/m^3) and h_{w300} (J/kg) is the wall enthalpy at 300 K. This method is limited to v_1 of 1828.8 m/s up to 7924.8 m/s and density ratio ρ_1/ρ_o from $8{\cdot}10^{-5}$ until 1.

$$\dot{q_{dh}} = 1.1356 \cdot \left[\frac{865}{\sqrt{0.3048^{-1} \cdot R_{SV}}} \cdot \left(\frac{0.3048^{-1} \cdot v_1}{10^4} \right)^{3.15} \cdot \sqrt{\frac{\rho_1}{\rho_o}} \cdot \left(\frac{h_o - h_w}{h_o - h_{w300}} \right) \right]. \tag{34}$$

3.5 FAY-RIDDELL

At last, the method proposed by Fay and Riddell (1958) is shown below, it is also the only method that considers the thermodynamic equilibrium in a direct way to obtain the required variables and returns the heat flux $\dot{q_{fr}}$ in W/m^2, hence,

$$\dot{q_{fr}} = 0.76 \cdot Pr^{-0.6} \cdot (\rho_{\bar{2}}\mu_{\bar{2}})^{0.4} \cdot (\rho_w \mu_w)^{0.1} \cdot \sqrt{\frac{dv_2}{dx}} \cdot (h_{oe} - h_w) \cdot \left[1 + (Le^{0.52} - 1)\frac{h_D}{h_o e} \right], \tag{35}$$

if the stagnation temperature is close to 2500 K, a change can be made in Eq. 35 as demonstrated in the work of Ilich *et al.* (2017), for this case, the dissociation of nitrogen will not happen, therefore, Lewis number (Le) is equal to 1, and Eq. 35 becomes,

$$\dot{q_{fr}} = 0.76 \cdot Pr^{-0.6} \cdot (\rho_{\bar{2}}\mu_{\bar{2}})^{0.4} \cdot (\rho_w \mu_w)^{0.1} \cdot \sqrt{\frac{dv_2}{dx}} \cdot (h_{oe} - h_w). \tag{36}$$

Analysing Eq. 36, the density ρ_w (kg/m^3) and μ_w (kg/m·s) are properties evaluated in the wall of the SV, h_{oe} is the enthalpy found at the outer edge of the boundary layer in J/kg, therefore,

$$h_{oe} = h_{\bar{2}} + \frac{v_{\bar{2}}^2}{2}. \tag{37}$$

3.6 HEAT LOAD

The integration of any previously approximate method with respect to the trajectory time results in the heat load Q. To implement this, a trapezoidal rule can be used, so,

$$Q = \int_{t_i}^{t_f} \dot{q_w}\, dt \approx \Delta t \cdot \left(\frac{\dot{q_1}}{2} + \dot{q_2} + \dot{q_3} + ... + \frac{\dot{q_F}}{2} \right), \tag{38}$$

t_i and t_f are the initial and final time respectively, $\dot{q}_w$ is the heat flux as function of time. On the other side of Eq. 38, Δt is an increment of time in seconds and $\dot{q}_n$, n=1, 2, 3,..., F, are values of heat flux in every instant of the trajectory time. Assuming that the values of $\dot{q}_n$ are given in W/m^2, Q will be found in J/m^2.

4. RESULTS AND DISCUSSIONS

Figure 4 shows the validation of the streamline conditions from the Standard Atmosphere of 1976 (COESA, 1976). Other information such as enthalpy (h_1) and Mach number (M_1) are easily obtained from these data.

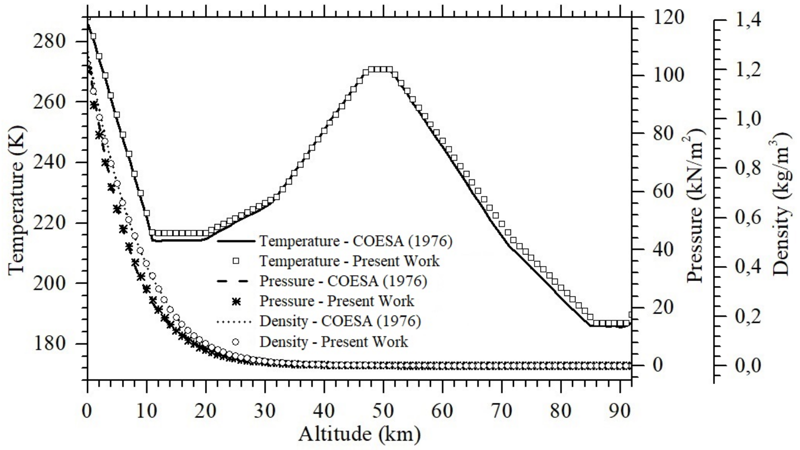

Figure 4. Validation of the data obtained through the U. S. Standard Atmosphere of 1976 (COESA, 1976).

Regarding the properties after the normal shock, Fig. 5 demonstrate a comparison between the pressure and temperature calculated from the perfect gas model and the thermodynamic equilibrium of 1987 (Srinivasan *et al.*, 1987).

The results considering the pressure were very close through the entire time that the normal shock was present, however, the maximum temperature generated with the perfect gas model exceeded the value of 30000 K at 85 km of altitude, this output is unrealistic, a proof of this is that the thermodynamic equilibrium of 1987 (Srinivasan *et al.*, 1987) returned 6060 K as the maximum value of temperature at 65 km of altitude.

The information in Fig. 5 is limited above 20 km because below this altitude the Mach number (M_1) becomes lower than 1. The increment of time used in Eq. 38 was 5 seconds, and the reason for this is that the most critical moment of heating in SARA's stagnation point is below 92 km (1500 s) of altitude, since the normal shock is no longer present around 20 km (1790 s), the time gap between these two points is 290 seconds, by using 5 seconds of increment it would give 58 points to calculate the all the results, this number of points is enough to create a good precision.

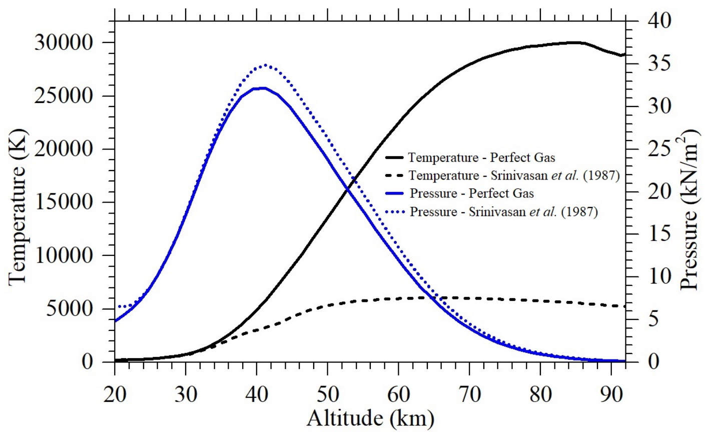

Figure 5. Comparison between the properties after the normal shock for the perfect gas model and thermodynamic equilibrium of 1987 (Srinivasan *et al.*, 1987).

4.1 HEAT FLUX

For the thermodynamic equilibrium, the heat capacity ratio is not constant as the perfect gas model, taking this into account Fig. 6 shows a comparison between this ratio ($\tilde{\gamma}$) for every thermodynamic equilibrium model used. One notable aspect in the behavior of the heat capacity ratio, is that as the $\tilde{\gamma}$ values get closer to 1.4 which is the value for the perfect gas model, the temperatures after the normal shock ($\tilde{T_2}$) for these models will also become closer to temperature T_2 obtained through the perfect gas (Fig. 5), all this happens at about 36 km.

The results for the heat fluxes (MW/m^2) with respect to the trajectory time (s) considering a wall temperature of 1000 K are shown in Fig. 7, where Detra-Hidalgo method presented the highest results among the approximate methods, and Van Driest the lowest. Therefore, at an altitude of 58 km (1660 s) the maximum and minimum values of heat flux were 1.99 MW/m^2 and 1.52 MW/m^2.

The numbers 1, 2, and 3 in the legend of the figures below represent the three thermodynamic equilibrium models used along with the Fay-Riddell approach. The number 1 stands for the model of 1972 (Tannehill and Mohling, 1972), 2 for 1974 (Tannehill and Mugge, 1974), and 3 for the model of 1987 (Srinivasan *et al.*, 1987).

The behavior of all the curves is very similar because all the approximate methods depend on the same properties of air before the stagnation point, therefore, this outcome is expected.

Still considering the wall temperature of 1000K, Tauber and Sutton-Graves approach showed results very close to each other as indicated in the red and blue curves. Even though Fay-Riddell method was evaluated using three different thermodynamic equilibrium models, no great differences were found in the heat fluxes, the reason behind this is that maybe SARA doesn't get exposed to extreme conditions where differences among these data would be able to be noticed.

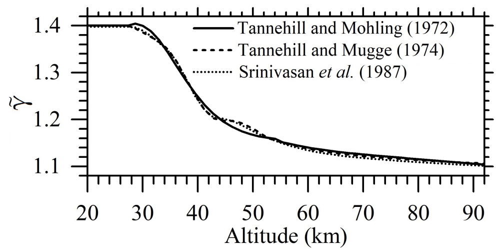

Figure 6. Variation of heat capacity ratio for every thermodynamic equilibrium model.

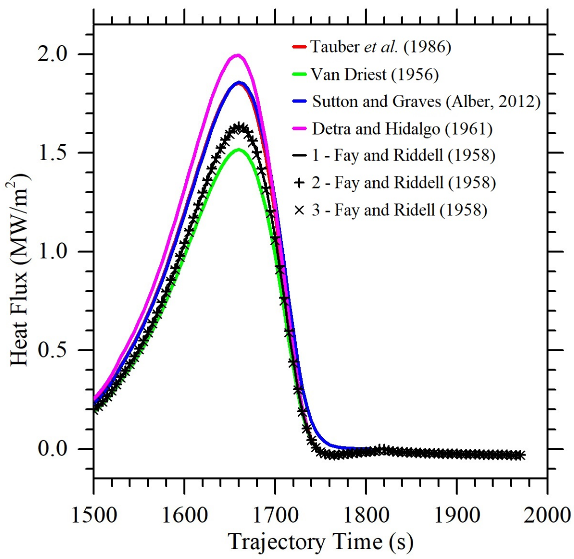

Figure 7. Approximate methods results for T_w = 1000K.

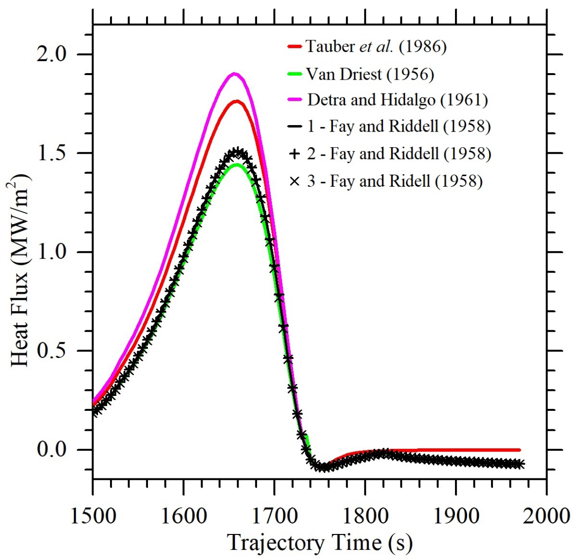

Figure 8. Approximate methods results for T_w = 2000K.

The same analysis can be done to the wall temperatures of 2000 K and 3000 K, where the maximum results between Detra-Hidalgo and Van Driest for T_w = 2000 K in Fig. 8 were 1.90 MW/m^2 and 1.44 MW/m^2 at 58 km (1660 s). Fig. 9 shows the results for T_w = 3000 K where the maximum value for Detra-Hidalgo was 1.77 MW/m^2 and for Van Driest 1.35 MW/m^2 at the same point of altitude.

Sutton-Graves results are not present in the last two wall temperatures because as stated before, this method is only valid for wall temperatures up to 1111 K. Nevertheless, no great differences were found between Fay-Riddell's approach in each specific wall temperature. The negative heat fluxes in all three wall temperatures after 1730 s (36 km) are explained by the fact that at that instant the temperature in the wall is higher than in the air ahead of the SARA frontal nose, thus, the heat transfer occurs in the opposite direction.

Something interesting to note is that considering the peak of heat flux, the Van Driest approach presented inferior results when compared with the Fay-Riddel method, which considered the dissociative effects of oxygen. This information is important because show how much these approximate methods are developed to present the most realistic situation.

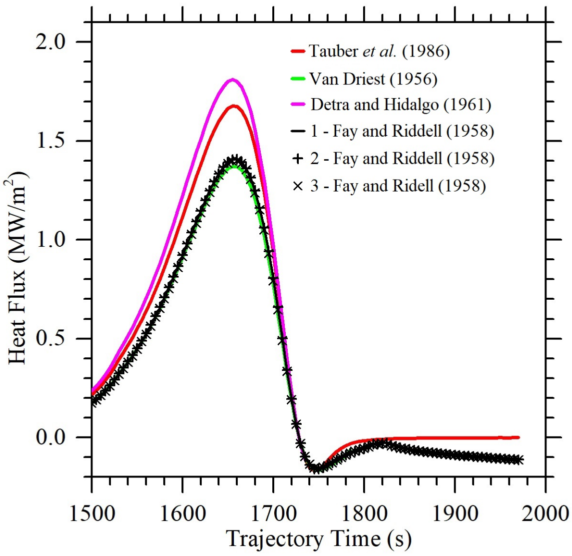

Figure 9. Approximate methods results for T_w = 3000K.

4.2 HEAT LOAD

Table 2 shows the heat loads obtained in every approximate method. As expected, Detra-Hidalgo's method presented the highest results in every wall temperature considered, where the maximum value found was 264.4 MJ/m^2 for a wall temperature of 1000 K. Fay-Riddell's method presented the lowest value with 157.7 MJ/m^2 when the wall temperature was 3000 K, where once again the effects of the dissociation of the oxygen take responsibility since a fraction of the energy is consumed to separate these molecules.

By analyzing any of these methods is possible to see that as the wall temperature increases, the heat load decrease in a proportional way, creating the idea that these properties are practically inversely proportional, and this happens because the heat transfer is always more prominent when there is a higher difference of temperature.

Table 2. Heat load values (MJ/m^2) for every approximate method.

Approximate Method	T_w = 1000 K	T_w = 2000 K	T_w = 3000 K
Tauber *et al.* (1986)	244.5	226.7	209.0
Van Driest (1956)	200.0	184.7	169.4
Sutton and Graves (Alber, 2012)	250.7	-	-
Detra and Hidalgo (1961)	264.0	248.1	232.2
1 - Fay and Riddell (1958)	214.4	191.9	172.4
2 - Fay and Riddell (1958)	214.8	192.3	172.7
3 - Fay and Riddell (1958)	208.9	181.8	157.7

5. CONCLUSION

The methods presented in this work should be used to create an initial analysis about the aerodynamic heating in a SV in order to develop a TPS. If safety is the most important matter, Detra-Hidalgo method must be adopted since dealing with the highest values of heating will automatically counter inferior ones, in any case, other factors must receive attention such as the heating caused through radiation, this topic was not taken into account in this work because SARA does not achieve great values of velocity where radiation heating would be dangerous to the SV structure.

It was possible to see that models such as the perfect gas do not fit for the determination of the properties of air at high temperatures, in this case, other models that consider the dissociation and ionization of air must be consulted, such as the three thermodynamic equilibrium present in this work.

If in a given project stage what is request is to have a notion about the aerodynamic heating at the stagnation point, the Tauber method should be used, since its implementation is simple and does not require the use of any thermodynamic equilibrium model. Also, this approach has no limitation on wall temperatures.

6. ACKNOWLEDGEMENTS

The first author gratefully acknowledge the financial support from Fundação Araucária de Apoio ao Desenvolvimento Científico e Tecnológico in form of scientific initiation scholarship.

The authors would like to acknowledge Fundação Araucária de Apoio ao Desenvolvimento Científico e Tecnológico, which provide a financial support under Grant 376/2014.

7. REFERENCES

Alber, I.E., 2012. *Aerospace engineering on the back of an envelope.* Springer, Berlin.

Anderson Junior, J.D., 2003. *Modern compressible flow: with a historical perspective.* McGraw-Hill, New York, 3rd edition.

Anderson Junior, J.D., 2006. *Hypersonic and high temperature gas dynamics.* AIAA, Reston, 2nd edition.

Chapman, S.J., 2018. *Fortran for scientists and engineers.* McGraw-Hill, New York, 4th edition.

COESA, 1976. "U.S. Standard atmosphere 1976". U.S. Government Printing Office, Washington, D. C.

Detra, R.W. and Hidalgo, H., 1961. "Generalized heat transfer formulas and graphs for nose cone re-entry into the atmosphere." *ARSJ*, Vol. 31, No. 3, pp. 318–321.

Fay, J.A. and Riddell, F.R., 1958. "Theory of stagnation point heat transfer in dissociated air." *JAS*, Vol. 25, No. 2, pp. 73–85.

Ilich, Z., Grossir, G. and Chazot, O., 2017. "Evaluation of the stagnation-point velocity gradient in low-enthalpy hypersonic flows." In *33rd AIAA Aerodynamic Measurement Technology and Ground Testing Conference - AIAA 2017-3984*. Denver, CO, United States.

Regan, F.J. and Anandakrishnan, S.M., 1993. *Dynamics of atmospheric re-entry.* AIAA, Washington, D.C.

Srinivasan, S., Tannehill, J.C. and Weilmuenster, K.J., 1987. "Simplified curve fits for the thermodynamic properties of equilibrium air." National Space and Aeronautics Administration, Washington, D. C.

Tannehill, J.C. and Mohling, R.A., 1972. "Development of equilibrium air computer programs suitable for numerical computation using time-dependent or shockcapturing methods." National Space and Aeronautics Administration, Washington, D. C.

Tannehill, J.C. and Mugge, P.H., 1974. "Improved curve fits for the thermodynamic properties of equilibrium air suitable for numerical computation using timedependent or shock-capturing methods." National Space and Aeronautics Administration, Washington, D. C.

Tauber, M.E., Menees, G.P. and Adelman, H.G., 1986. "Aerothermodynamics of transatmospheric vehicles." Paper 86-1257, AIAA/ASME 4th Joint Thermophysics and Heat Transfer Conference, United States, Boston, MA, Deposit: June, 1986.

Toro, P.G.P., Minucci, M.A.S. and Chanes, J.B.J., 2004. "Experimental hypersonic investigation over the micro-satellite sara". In *Proceedings of the 10th Brazilian Congress of Thermal Sciences and Engineering - ENCIT 2004*. Rio de Janeiro, RJ, Brazil.

Van Driest, E.R., 1956. "The problem of aerodynamic heating." *Aeronautical Engineering Review*, Vol. 15, No. 10, pp. 26–41.

8. RESPONSIBILITY NOTICE

The authors Filipe Eduardo da Silva and Francisco Augusto Aparecido Gomes are solely responsible for the printed material included in this paper.